International Journal of Mathematics and Computer Research
ISSN: 2320-7167
Volume 10 Issue 08 August 2022, Page no. – 2866-2879
Index Copernicus ICV: 57.55, Impact Factor: 7.362
DOI: 10.47191/ijmcr/v10i8.08

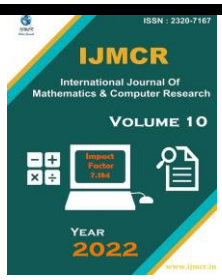

Modelling Blood Flow through a Sclerotic Artery and the Effect of Thermal Heat on Cholesterol Concentration in the Presence of a Magnetic Field

K. W. Bunonyo[1], L. Ebiwareme [2]
[1]Department of Mathematics and Statistics, Federal University Otuoke, Nigeria
[2]Department of Mathematics, Rivers State University, Nigeria

ARTICLE INFO

Published Online:
31 August 2022

Corresponding Authors:
K. W. Bunonyo

ABSTRACT

Blood flow through a sclerotic artery and the effect of thermal heat on cholesterol concentration in the presence of a magnetic field are modelled using mathematical models which represent the blood momentum coupled with buoyancy due to temperature, cholesterol concentration, porosity of the medium and magnetic field effect. The study involved the formulation of the geometry of atherosclerosis at a specific location with sclerosis over time in the arterial channel. The system of equations was solved using the Laplace method, where the blood velocity, cholesterol concentration and temperature profile were obtained with governing parameters such as magnetic field, Schmidt number, Soret number, Prandtl number, radiation parameter, chemical parameter, and oscillatory frequency, respectively. The result revealed that the blood velocity increases for different units of increase in Soret number, radiation parameter, and porosity parameter, while the velocity decreases for different values of solutal Grashof number, Schmidt number, Prandtl number, and magnetic field parameter. Furthermore, the cholesterol concentration decreases with an increase in Soret number, Schmidt number, and Prandtl number, respectively. The study also revealed that an increase in Prandtl number, radiation parameter, and oscillatory frequency parameter decreases the blood temperature.

KEYWORDS: Blood, Modelling, Sclerotic Artery, Cholesterol, Concentration, Thermal Heat, Magnetic Field.

INTRODUCTION

Modelling blood flow through sclerotic arteries is considered to be of immense benefit concerning many cardiovascular diseases. The poor circulation of blood in the human body due to occlusion in arteries causes major health risks. Arteries carry oxygenated blood with nutrients from the heart to each cell and tissue of the body in the circulatory system of the human body. Atherosclerosis, or stenosis, is one of the leading causes of death in most developing countries. There is significant evidence that vascular fluid mechanics plays a leading role in the progression and development of arterial sclerosis, which is one of the most common diseases in mammals. The haemodynamic study of blood flow in arteries allows some significant aspects due to the feasible medical applications as well as the bioengineering interest. The hemodynamic nature of the blood flow is determined by the occurrence of arterial atherosclerosis. According to Sharma *et al.* [1], normal blood flow in the presence of stenosis in an artery is disturbed. The investigation of the pulsatile blood flow through a sclerotic artery is motivated by the need to obtain a better understanding of the influence of flow phenomena on stroke and atherosclerosis. The rate at which kidney cells execute the regulation of the volume of water or salts in the body is affected by using drugs; similarly, the rate at which blood flows through arteries may also be affected or slowed down by the drugs. It is important to note that there is a significant difference between restoration and reparation. By the application of drugs, the damaged structures or functions of a human body can be repaired but not restored. There have been several investigations by researchers into the study of various aspects of blood circulation in normal diseased arteries having single stenosis according to Bunonyo and Amos [2]. Blood flow characteristics through an artery in the presence of multi-stenosis were developed by Chakravarty and Sannigrahi [3]. The investigation of basic biofluid dynamics problems attracts interest due to the numerous proposed applications in bioengineering and medical sciences. The study of bio-fluids under the presence

of magnetic fields with dissipation finds its applications in various upcoming fields like innovative drug targeting, surgical operations etc. Magnetic therapy and blood vessels dilated with the use of its induced heat can be used as an alternative method for cancer therapy and other medical treatments Abdoullahzadeh *et al*. [4]. In these medical functions, vessel wall cooling is proposed as an efficient approach to sustaining the living conditions of the blood. Haik *et al*. [5] reported a 30% decrease in blood flow rate when subjected to a high magnetic field of 10 T, while Yadav *et al*. [6] showed a similar reduction in blood flow rate but at a much smaller magnetic field of 0.002 T. A theoretical analysis of blood flow and heat transfer in a permeable vessel in the presence of an external magnetic field has been discussed by Sinha *et al*. [7]. Shit and Roy [8] studied the effects of an induced magnetic field on blood flow through a constricted channel and demonstrated that increasing the values of the magnetic field reduces the velocity of the blood flow at the centre.

Heat transfer in blood has so many practical applications in muscle and skin tissues, thermal therapy etc. In the past decades, there have been a number of studies to test heat transfer in blood vessels. Barcroft and Edholm [9] considered the effect of temperature on blood flow and deep temperature in the human forearm. Considering the heat and mass transfer of blood flow considering its pulsatile hydro-magnetic rheological nature under the presence of viscous dissipation, Joule heating, and a finite heat source discussed by Sharma *et al*. [10]. The purpose of thermal radiation is to improve control of disease while preserving a good quality of life. Thermal radiation is one of the methods applied by medical practitioners to ease cardiovascular diseases. The process involves carrying heat below the skin surface into tissues and muscles. Deep heat speeds up healing and cuts down on plaque deposition, conducting to increased blood flow, as reported by Zee [11]. Ma *et al*. [12] stated that thermal radiation is the most commonly used energy in living cells for keeping and handling cardiovascular diseases and rebuilding connective tissue. Sinha and Shit [13] have investigated the combined effects of thermal radiation and MHD heat transfer on blood flow through a capillary. Sharma and Gaur [14] studied the effect of variable viscosity on chemically reacting magneto-blood flow with heat and mass transfer. Recently, Sharma and Gaur [15] analysed the arterial catheterization (widening of arteries by a balloon in the presence of mild stenosis) in the presence of thermal radiation.[16] investigated tumour temperature heterogeneity during hyperthermia due to irregular tumour vascular perfusion. They compared temperature distributions in human tumours subjected to superficial hyperthermia under conditions of normal and occluded blood flow. Three patients with recurrent malignant melanoma on the leg were treated with radiation followed by hyperthermia 60-90 min later on days 1, 8, and 22. Heating (15-30 min) with normal blood flow was followed by 15 min of heating with tourniquet occlusion. Hyperthermia was delivered using either a 1.4 MHz ultrasound or a 915 MHz microwave applicator. Temperatures were monitored using superficial and interstitial thermometers in tumor and normal tissues. These studies demonstrate directly that the temperature heterogeneity that exists in human tumours subjected to external heating can be reduced by occluding the blood supply. Ponalagusamy & Selvi [17] presented a paper that sheds some light on a mathematical model for blood flow through stenosed arteries with axially variable peripheral layer thickness and variable slip at the wall. The model consists of a core region of suspension of all the erythrocytes assumed to be a Casson fluid and a peripheral layer of plasma as a Newtonian fluid where the peripheral layer thickness and slip velocity are assumed a priori based on experimental observations. Hanvey and Bunonyo [18] carried out an investigation into the influence of treatment parameters on the flow of blood in a stenosed artery in the presence of a magnetic field with heat transfer. They solved the momentum equation governing by scaling it to a dimensionless structure with the aid of some dimensionless parameters. The equations have been analytically solved using the modified Bessel equation and by the method of undetermined coefficients in order to obtain the temperature profile and velocity profile of the blood flow. The model analysis and results are presented graphically with the help of the software Mathematica. Moreover, the velocity of the blood is adopting a wavy pattern as the values of the parameters vary. The study can be useful in providing a perception of the treatment caused by the superfluous consumption of fatty foods, thus decreasing the risk of cancer, hypertension, and many heart-related diseases. Hanvey [19] studied blood flow between two plate channels with the effect of heat transfer and mass transfer. An inclined magnetic field has been applied to the parallel plates filled with porous substances. The partial differential equations that govern the flow field have been resolved numerically by applying non-dimensional parameters. The effect of the inclination of the magnetic field on the parallel plate channel has been analyzed. Kubugha and Amos [20] used a mathematical model to investigate LDL-C and blood flow through an inclined channel with heat in the presence of a magnetic field. In their research, mathematical models were formulated to represent LDL-C and blood flow and energy transfer as a coupled system of partial differential equations (PDEs). The PDEs were scaled using the dimensionless quantities to dimensionless partial differential equations. They further reduced the equations to ordinary differential equations (ODEs) using the perturbation method involving the oscillatory term. Thereafter, governing equations are solved directly using the method of undetermined coefficient.

OBJECTIVE OF THE PRESENT RESEARCH

The object of this research is to formulate models to investigate blood flow through a sclerotic artery with the effect of thermal heat on cholesterol concentration in the presence of a magnetic field, which was not considered in [17-22]. The objective model is a nonlinear, incompressible momentum equation, coupled with the cholesterol concentration and thermal heat energy in the presence of a magnetic field. The accompanying models are cholesterol concentration and thermal energy models. Linear partial differential equations will be used to solve the momentum equation. The study shall involve the formulation of the geometry of atherosclerosis with exponential growth and treatment at a specific location over time in the arterial channel. The system of equations shall be solved using the Laplace method, where we are expected to obtain blood velocity, temperature, and cholesterol concentration equations; in addition, numerical simulation shall be carried out to investigate the impact of some of the governing parameters on the blood velocity, cholesterol concentration, and blood temperature profiles, respectively; thereafter, drawing conclusions from the results and discussions.

Mathematical formulation

We consider blood to be non-Newtonian, electrically conducting, and incompressible viscous fluid, flowing through an atherosclerotic artery presumed to be a cylindrical channel with a velocity $w^*\left(r^*, x^*\right)$, where r^* and x^* indicating the direction of the flow, and it's saturated with cholesterol, with an exponential growth rate. The flow in the vertical direction is not considered hence, it is zero. The pressure gradient is in the horizontal direction and is being generated by the ventricular action, and perpendicular applied magnetic field is also considered. In view of aforementioned consideration, and following Bunonyo and Ebiwareme [21], we present the models governing the flow as:

The geometry of atherosclerosis

$$R=\begin{cases} R_0-\dfrac{\delta^*}{2}\left(1+cos\dfrac{2\pi x^*}{\lambda^*}\right) & \text{at } d_0\le x^*\le\lambda^* \\ R_0 & \text{at } 0\le x^*\le d_0 \end{cases} \tag{1}$$

$$\text{where } x^*=\left(d_0+\frac{\lambda^*}{2}\right) \tag{2}$$

Blood Momentum Equation

$$\rho_b\frac{\partial w^*}{\partial t^*}=-\frac{\partial P^*}{\partial x^*}+\mu_b\left(\frac{\partial^2 w^*}{\partial r^{*2}}+\frac{1}{r^*}\frac{\partial w^*}{\partial r^*}\right)-\frac{\mu_b\varphi}{k^*}w^*-\sigma B_0^2 w^*+\rho_b g\beta_T\left(T^*-T_\infty\right)+\rho_b g\beta_C\left(C^*-C_\infty\right) \tag{3}$$

Heat Equation

$$\rho_b c_b\frac{\partial T^*}{\partial t^*}=k_{Tb}\left(\frac{\partial^2 T^*}{\partial r^{*2}}+\frac{1}{r^*}\frac{\partial T^*}{\partial r^*}\right)-Q_0\left(T^*-T_\infty\right) \tag{4}$$

Cholesterol Concentration Equation

$$\frac{\partial C^*}{\partial t^*}=D_m\left(\frac{\partial^2 C^*}{\partial r^{*2}}+\frac{1}{r^*}\frac{\partial C^*}{\partial r^*}\right)+\frac{D_T k_T}{T_m}\left(\frac{\partial^2 T^*}{\partial r^{*2}}+\frac{1}{r^*}\frac{\partial T^*}{\partial r^*}\right) \tag{5}$$

The corresponding initial and boundary conditions are

$$\left.\begin{aligned} w^*=0, T^*=T_w, C^*=C_w \quad \text{at } r^*=R \\ w^*\neq 0, T^*\neq T_\infty, C^*\neq C_\infty \quad \text{at } r^*=0 \end{aligned}\right\} \tag{6}$$

Dimensionless Parameters

$$\left.\begin{aligned} &x=\frac{x^*}{\lambda^*}, r=\frac{r^*}{R_0}, t=\frac{t^*\upsilon_b}{R_0^2}, w=\frac{w^*R_0}{\upsilon_b}, Gr=\frac{g\beta_T\left(T_w-T_\infty\right)R_0^3}{\upsilon_b^2}, \theta=\frac{T^*-T_\infty}{T_w-T_\infty}, S_r=\frac{D_T k_{Tb}}{\upsilon_b T_m}\left(\frac{T_w-T_\infty}{C_w-C_\infty}\right), \\ &Rd_1=\frac{Q_0R_0^2}{\mu_b c_b}, Gc=\frac{g\beta_C\left(C_w-C_\infty\right)R_0^3}{\upsilon_b^2}, M=B_0R_0\sqrt{\frac{\sigma}{\mu_b}}, \frac{1}{k}=\frac{\varphi R_0^2}{k^*}, Sc=\frac{\upsilon_b}{D_m}, \delta^*=\frac{\delta R_0 e^{at}}{R_T}, \\ &Pr=\frac{\mu_b c_b}{k_{Tb}}, P=\frac{R_0^3P^*}{\lambda^*\mu_b\upsilon_b}, \phi=\frac{C^*-C_\infty}{C_w-C_\infty}, \frac{\delta}{R_0}\ \square\ 1 \end{aligned}\right\} \tag{7}$$

Applying the Dimensionless parameters in equation (7), equations (1)-(6) are reduced to

$$\frac{R}{R_0}=\begin{cases}1-\dfrac{\delta}{2R_T}e^{at}\left(1+cos2\pi x\right) & \text{at } d_0\le x^*\le\lambda^*\\ 1 & \text{at } 0\le x^*\le d_0\end{cases} \tag{8}$$

Where $x=\dfrac{1}{\lambda}\left(d_0+\dfrac{\lambda}{2}\right)$ (9)

$$\frac{\partial w}{\partial t}=-\frac{\partial P}{\partial x}+\left(\frac{\partial^2 w}{\partial r^2}+\frac{1}{r}\frac{\partial w}{\partial r}\right)-\frac{1}{k}w-M^2w+Gr\theta+Gc\phi \tag{10}$$

$$Pr\frac{\partial\theta}{\partial t}=\left(\frac{\partial^2\theta}{\partial r^2}+\frac{1}{r}\frac{\partial\theta}{\partial r}\right)-Rd_1Pr\theta \tag{11}$$

$$Sc\frac{\partial\phi}{\partial t}=\left(\frac{\partial^2\phi}{\partial r^2}+\frac{1}{r}\frac{\partial\phi}{\partial r}\right)+S_rSc\left(\frac{\partial^2\theta}{\partial r^2}+\frac{1}{r}\frac{\partial\theta}{\partial r}\right) \tag{12}$$

The corresponding initial and boundary conditions are

$$\left.\begin{aligned}&w\neq 0,\theta\neq 0,\phi\neq 0 \text{ at } r=0\\ &w=0,\theta=1,\phi=1 \text{ at } r=\frac{R}{R_0}\end{aligned}\right\} \tag{13}$$

Reduction to Ordinary Differential Equation

Since the pressure is generated by the ventricular action, we can reduce the partial differential equations (PDEs) in equations (10)-(12) to a coupled system of ordinary differential equations (ODEs) using the following:

$$\left.\begin{aligned}&w(r,t)=w_0(r)e^{i\omega t},\theta(r,t)=\theta_0(r)e^{i\omega t}\\ &\phi(r,t)=\phi_0(r)e^{i\omega t},-\frac{\partial P}{\partial x}=P_0e^{i\omega t}\end{aligned}\right\} \tag{14}$$

Using equation (14) in reducing the PDE, we have the ODEs as follows:

$$\frac{d^2w_0}{dr^2}+\frac{1}{r}\frac{dw_0}{dr}-\beta_1^2w_0=P_0-Gr\theta_0-Gc\phi_0 \tag{15}$$

$$\frac{d^2\theta_0}{dr^2}+\frac{1}{r}\frac{d\theta_0}{dr}-\beta_2^2\theta_0=0 \tag{16}$$

$$\frac{d^2\phi_0}{dr^2}+\frac{1}{r}\frac{d\phi_0}{dr}-\beta_4^2\phi_0=-S_rSc\left(\frac{d^2\theta_0}{dr^2}+\frac{1}{r}\frac{d\theta_0}{dr}\right) \tag{17}$$

where $\beta_1^2=\left(\dfrac{1}{k}+M^2+i\omega\right),\beta_2^2=\left(Rd_1+i\omega\right)Pr,\beta_4^2=Sci\omega$

The corresponding initial and boundary conditions are

$$\left.\begin{aligned}&w_0\neq 0,\theta_0\neq 0,\phi_0\neq 0 \quad \text{at } r=0\\ &w_0=0,\theta_0=e^{-i\omega t},\phi_0=e^{-i\omega t} \text{ at } r=\frac{R}{R_0}\end{aligned}\right\} \tag{18}$$

METHOD OF SOLUTION

We would adopt the Laplace method in solving the perturbed governing models in equations (15)-(17) subject to the boundary conditions in equation (18), which are:

$$L\{w_0(r)\} = w_0(s) = \int_0^\infty w_0(r)e^{-rs}dr \tag{19}$$

$$L\{\theta_0(r)\} = \theta_0(s) = \int_0^\infty \theta_0(r)e^{-rs}dr \tag{20}$$

$$L\{\phi_0(r)\} = \phi_0(s) = \int_0^\infty \phi_0(r)e^{-rs}dr \tag{21}$$

Retransforming equation (16), we have

$$\frac{d^2\theta_0}{dr^2} + \frac{1}{r}\frac{d\theta_0}{dr} + \beta_{21}^2\theta_0 = 0 \tag{22}$$

where $\beta_{21} = i\beta_2$, and applying equation (20) on equation (22), we have:

$$L\left\{r\frac{d^2\theta_0}{dr^2}\right\} + L\left\{\frac{d\theta_0}{dr}\right\} + \beta_{21}^2 L\{r\theta_0\} = 0 \tag{23}$$

Simplifying equation (23), we have

$$L\left\{r\frac{d^2\theta_0}{dr^2}\right\} + L\left\{\frac{d\theta_0}{dr}\right\} + \beta_{21}^2 L\{r\theta_0\} = 0 = -\frac{d}{ds}\left(s^2\theta_0(s) - s\theta_0(0) - \dot{\theta}_0(0)\right) + s\theta_0(s) - \theta_0(0) - \beta_{21}^2\frac{d\theta_0}{ds} \tag{24}$$

Simplifying equation (24), we have

$$\frac{d\theta_0}{ds} + \frac{s}{\left(s^2 + \beta_{21}^2\right)}\theta_0(s) = 0 \tag{25}$$

Solving equation (25), we have

$$\theta_0(r) = B_2 I_0(\beta_2 r) \tag{26}$$

Note that $J_0(i\beta_2 r) = I_0(\beta_2 r)$, so that the solution of equation (28) is

Solving for the constant coefficient in equation (26), we have:

$$\theta_0(r) = \left(\frac{e^{-i\omega t}}{I_0(\beta_2 h)}\right) I_0(\beta_2 r) \tag{27}$$

Substitute equation (27) into equation (14), we have

$$\theta(r,t) = \left(\left(\frac{e^{-i\omega t}}{I_0(\beta_2 h)}\right) I_0(\beta_2 r)\right) e^{i\omega t} \tag{28}$$

Differentiate equation (27) twice and substitute the result into equation (17), we have

$$\frac{d^2\phi_0}{dr^2} + \frac{1}{r}\frac{d\phi_0}{dr} - \beta_4^2\phi_0 = -\frac{S_r Sc e^{-i\omega t}}{I_0(\beta_2 h)}\left(\beta_2^2 + \frac{16\beta_2^4 r^2}{64} + \frac{36\beta_2^6 r^4}{2304} + \ldots\right) \tag{29}$$

The homogenous part of equation (29) is:

$$\frac{d^2\phi_0}{dr^2} + \frac{1}{r}\frac{d\phi_0}{dr} + \beta_{41}^2\phi_0 = 0 \tag{30}$$

where $\beta_{41} = i\beta_4$, and applying equation (21) on equation (30), then:

$$L\left\{r\frac{d^2\phi_0}{dr^2}\right\} + L\left\{\frac{d\phi_0}{dr}\right\} + \beta_{41}^2 L\{r\phi_0\} = 0 \tag{31}$$

Simplifying equation (31), we have

$$L\left\{r\frac{d^2\phi_0}{dr^2}\right\} + L\left\{\frac{d\phi_0}{dr}\right\} + \beta_{41}^2 L\{r\phi_0\} = 0 = -\frac{d}{ds}\left(s^2\phi_0(s) - s\phi_0(0) - \dot{\phi}_0(0)\right) + s\phi_0(s) - \theta_0(0) - \beta_{41}^2\frac{d\phi_0}{ds} \tag{32}$$

Simplifying equation (32), we have:

$$\frac{d\phi_0}{ds}+\frac{s\phi_0}{\left(s^2+\beta_{41}^2\right)}=0 \tag{33}$$

Solving equation (33), we have:

$$\phi_0\left(r\right)=\left(\frac{e^{-i\omega t}}{I_0\left(\beta_4 h\right)}\right)I_0\left(\beta_4 r\right) \tag{34}$$

The particular solution to equation (29), which is:

$$\phi_{0p}\left(r\right)=A_1+A_2r^2+A_3r^4 \tag{35}$$

The solution of equation (29) is:

$$\phi_0\left(r\right)=A_0I_0\left(\beta_4 r\right)+A_1+A_2r^2+A_3r^4 \tag{36}$$

The cholesterol concentration equation is

$$\phi\left(r,t\right)=\left(A_0I_0\left(\beta_4 r\right)+A_1+A_2r^2+A_3r^4\right)e^{i\omega t} \tag{37}$$

Substitute equation (36) and (27) into equation (15), which is

$$\frac{d^2w_0}{dr^2}+\frac{1}{r}\frac{dw_0}{dr}-\beta_1^2w_0=\left[\begin{array}{l}P_0-A_1Gc-\left(\dfrac{Gre^{-i\omega t}}{I_0\left(\beta_2 h\right)}\right)\left(1+\dfrac{\beta_2^2r^2}{4}+\dfrac{\beta_2^4r^4}{64}+\dfrac{\beta_2^6r^6}{2304}+\ldots\right)\\-\left(GcA_0I_0\left(\beta_4 r\right)+A_2Gcr^2+A_3Gcr^4\right)\end{array}\right] \tag{38}$$

Applying equation (19) on the homogenous part of equation (38), we have:

$$L\left\{r\frac{d^2w_0}{dr^2}\right\}+L\left\{\frac{dw_0}{dr}\right\}+\beta_{11}^2L\left\{rw_0\right\}=0 \tag{39}$$

Simplifying equation (39), we have

$$L\left\{r\frac{d^2w_0}{dr^2}\right\}+L\left\{\frac{dw_0}{dr}\right\}+\beta_{11}^2L\left\{rw_0\right\}=0=-\frac{d}{ds}\left(s^2w_0\left(s\right)-sw_0\left(0\right)-\dot{\theta}_0\left(0\right)\right)+sw_0\left(s\right)-w_0\left(0\right)-\beta_{11}^2\frac{dw_0}{ds} \tag{40}$$

Simplifying equation (40), we have

$$\frac{dw_0}{ds}+\frac{s}{\left(s^2+\beta_{11}^2\right)}w_0\left(s\right)=0 \tag{41}$$

Solving equation (41), we have:

$$w_{0h}\left(r\right)=L^{-1}\left\{\frac{B_3}{\sqrt{\left(s^2+\beta_{11}^2\right)}}\right\}=B_3L^{-1}\left\{\frac{1}{\sqrt{\left(s^2+\beta_{11}^2\right)}}\right\}=B_3J_0\left(\beta_{11}r\right)=B_3J_0\left(i\beta_1 r\right) \tag{42}$$

The particular solution of equation (38) we have:

$$w_{0p}\left(r\right)=A_4+A_5I_0\left(\beta_2 r\right)+A_6I_0\left(\beta_4 r\right)+A_7r^2+A_8r^4 \tag{43}$$

Then the solution of equation (38) is the sum of equations (42) and (43), then:

$$w_0\left(r\right)=B_3I_0\left(\beta_1 r\right)+A_4+A_5I_0\left(\beta_2 r\right)+A_6I_0\left(\beta_4 r\right)+A_7r^2+A_8r^4 \tag{44}$$

Solving for the constant coefficient in equation (44), and substituting the results into equation (14), we have:

$$w\left(r,t\right)=\left(B_3I_0\left(\beta_1 r\right)+A_4+A_5I_0\left(\beta_2 r\right)+A_6I_0\left(\beta_4 r\right)+A_7r^2+A_8r^4\right)e^{i\omega t} \tag{45}$$

RESULTS

Numerical simulations are performed using the data values extracted from Bunonyo and Amos [2], Bunonyo and Ebiwareme [21] and Nessa *et al*. [22]

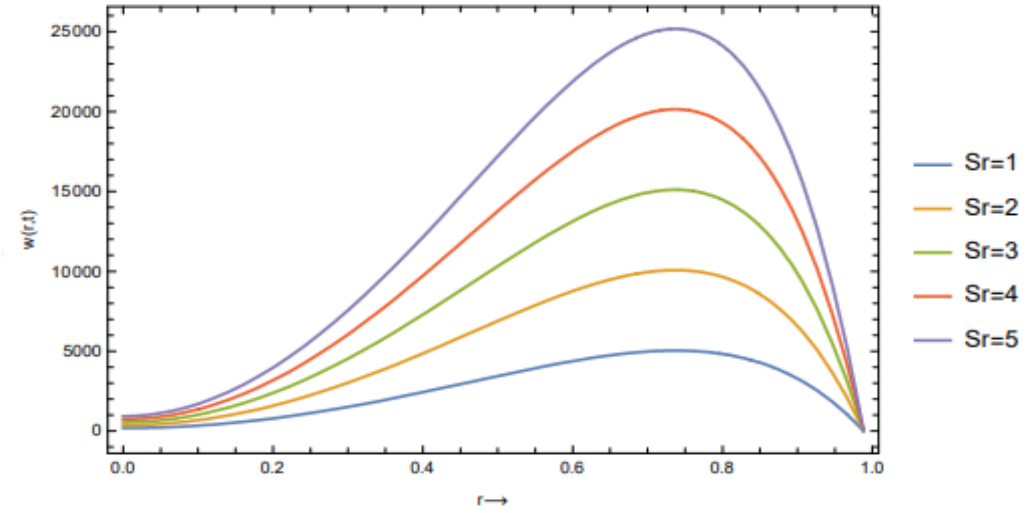

Fig 1. Plot Showing Blood Velocity for Different Soret Number with values

$Gc = 15, Pr = 2.1, Sc = 2, Rd_3 = 2, Rd_1 = 2, \omega = 0.3, k = 0.05, M = 1.5, x = 0.3$

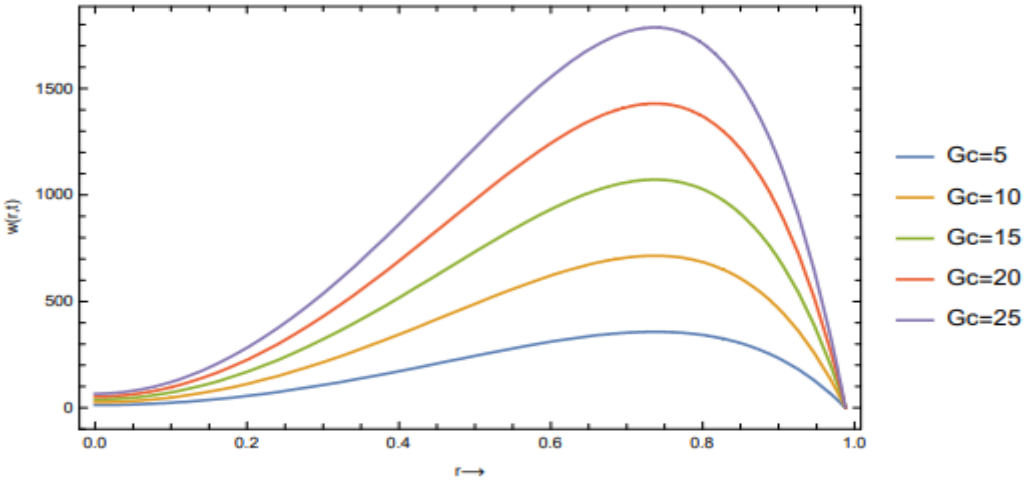

Fig 2. Plot Showing Blood Velocity for Different Grashof Number with values

$Sr = 2, Pr = 2.1, Sc = 0.2, Rd_3 = 2, Rd_1 = 2, \omega = 0.3, k = 0.05, M = 1.5, x = 0.3$

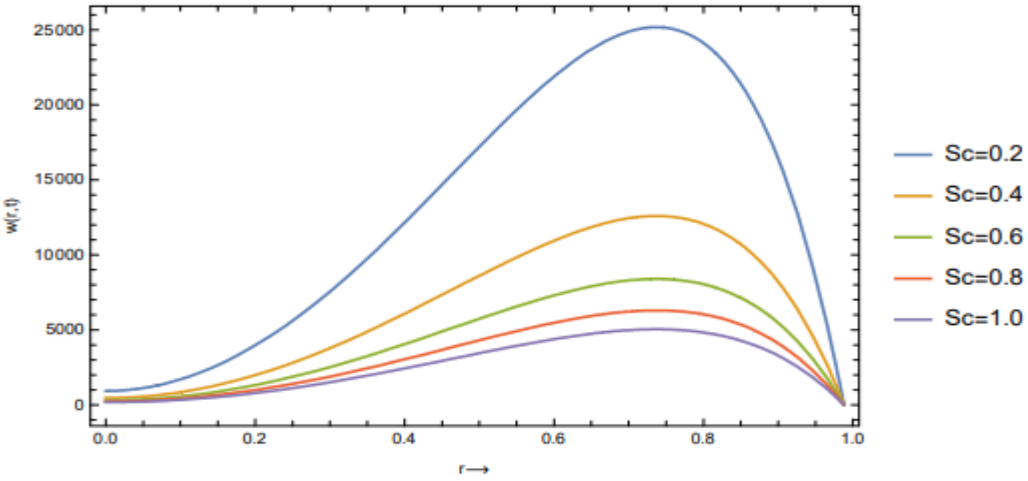

Fig 3. Plot Showing Blood Velocity for Different Schmidt Number with values

$Sr = 2, Gc = 15, Pr = 2.1, Rd_3 = 2, Rd_1 = 2, \omega = 0.3, k = 0.05, M = 1.5, x = 0.3$

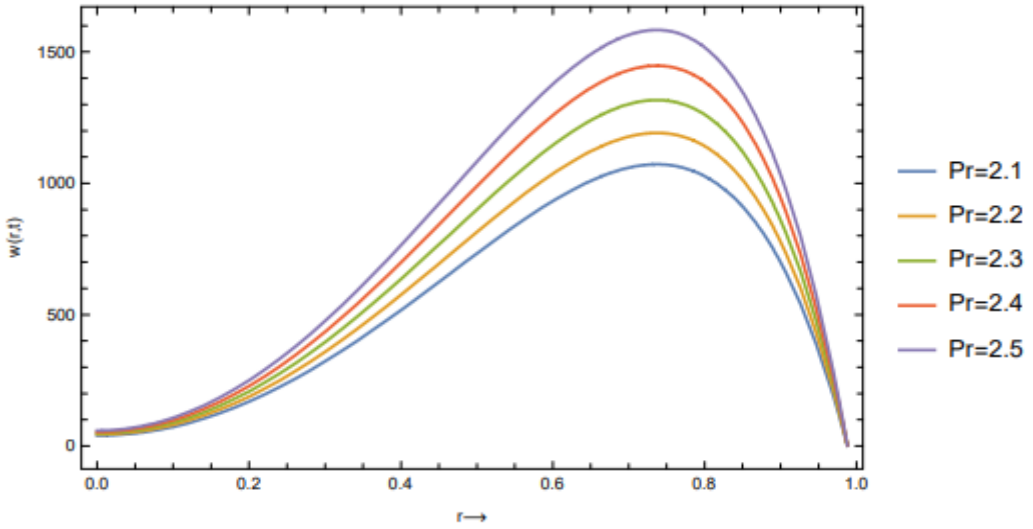

Fig 4. Plot Showing Blood Velocity for Different Prandtl Number with values

$Sr = 2, Gc = 15, Sc = 0.2, Rd_3 = 2, Rd_1 = 2, \omega = 0.3, k = 0.05, M = 1.5, x = 0.3$

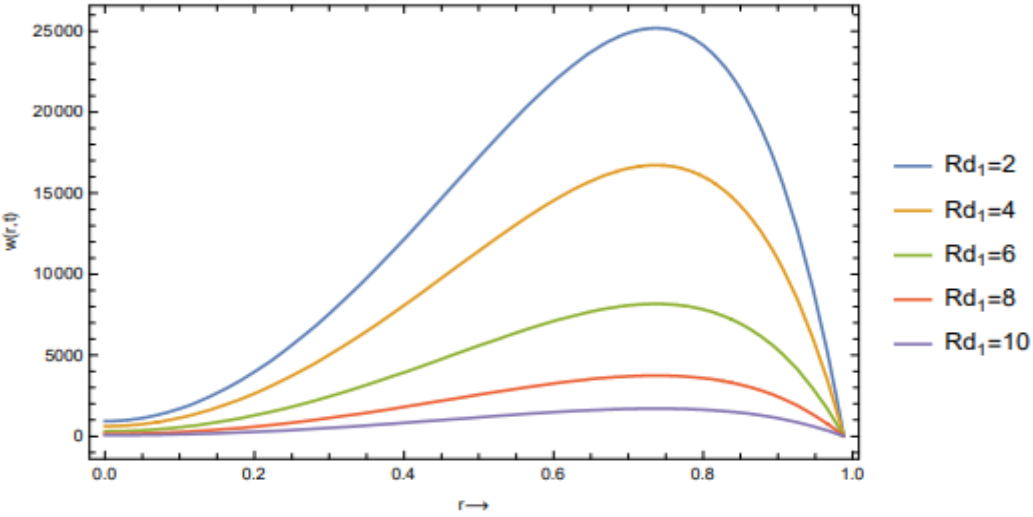

Fig 5. Plot Showing Blood Velocity for Different Radiation with values

$Sr = 2, Gc = 15, Pr = 2.1, Sc = 0.2, Rd_3 = 2, \omega = 0.3, k = 0.05, M = 1.5, x = 0.3$

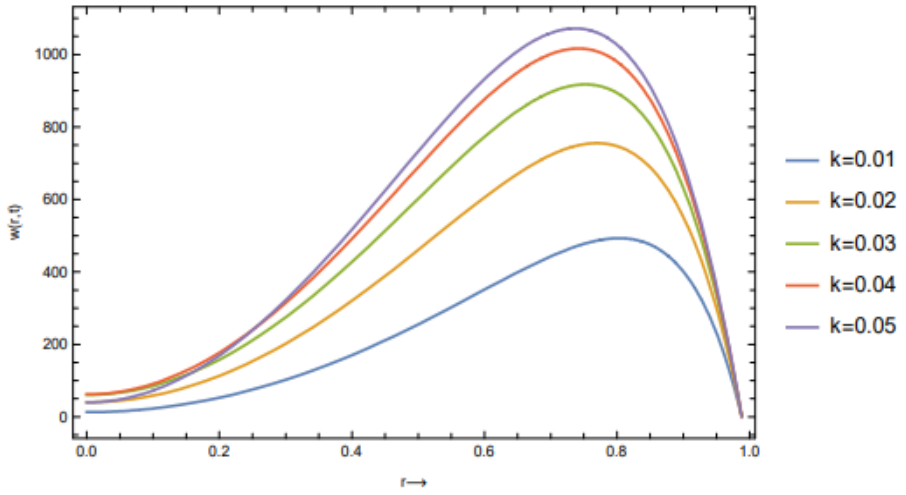

Fig 6.Plot Showing Blood Velocity for Different Porosity with values

$Sr = 2, Gc = 15, Pr = 2.1, Sc = 0.2, Rd_3 = 2, Rd_1 = 2, \omega = 0.3, M = 1.5, x = 0.3$

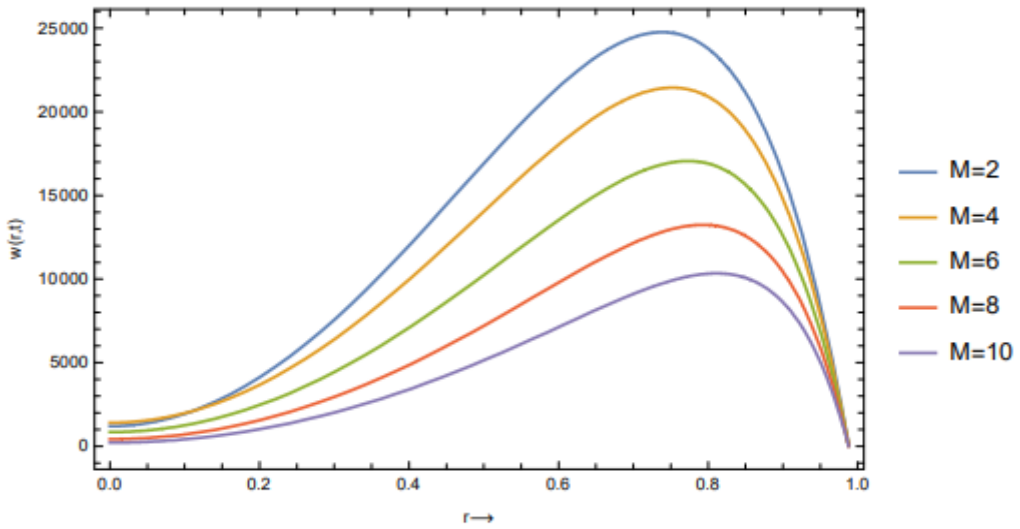

Fig 7.Plot Showing Blood Velocity for Different Magnetic Field with values

$Sr = 2, Gc = 15, Pr = 2.1, Sc = 0.2, Rd_3 = 2, Rd_1 = 2, \omega = 0.3, k = 0.05, x = 0.3$

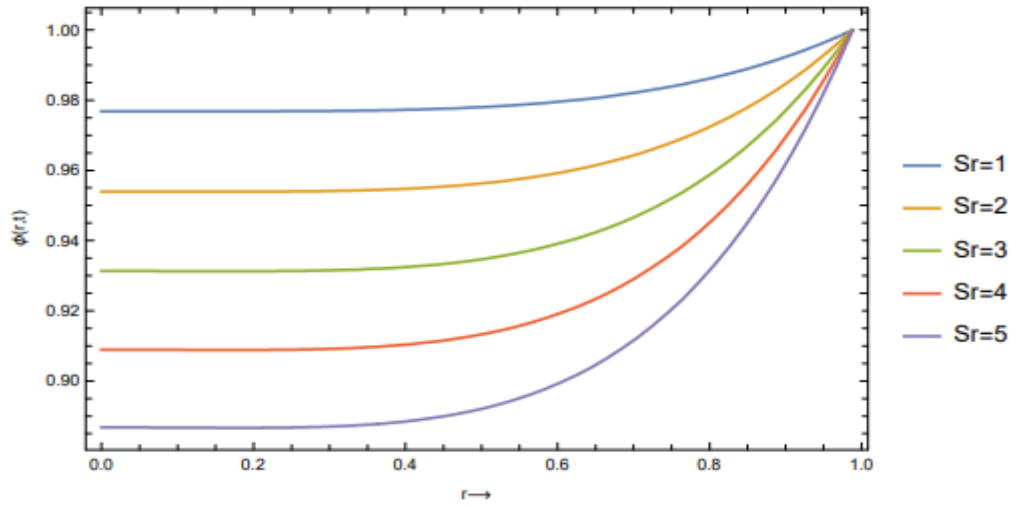

Fig 8. Plot Showing Cholesterol Concentration for Different Soret Number with values

$Pr = 2.1, Sc = 0.2, Rd_1 = 2, \omega = 0.3, x = 0.3$

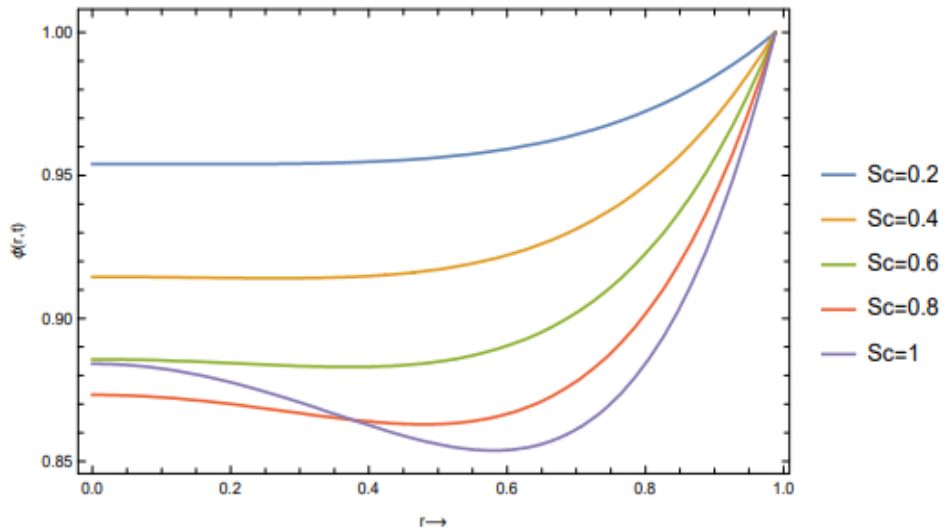

Fig 9. Plot Showing Cholesterol Concentration for Different Schmidt Number with values

$Pr = 2.1, Rd_1 = 2, \omega = 0.3, Sr = 2, x = 0.3$

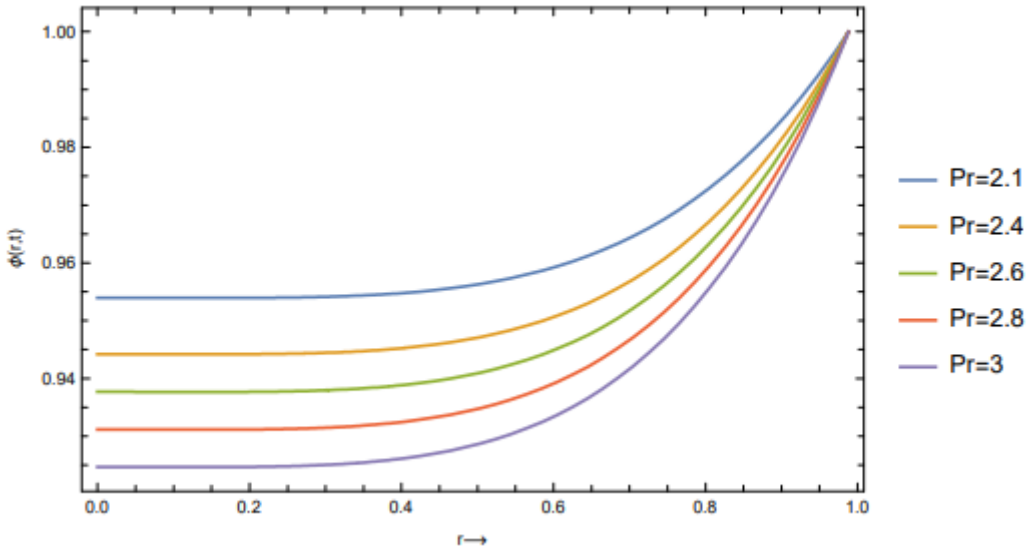

Fig 10. Plot Showing Cholesterol Concentration for Different Prandtl Number with values

$Sc = 0.2, Rd_1 = 2, \omega = 0.3, Sr = 2, x = 0.3$

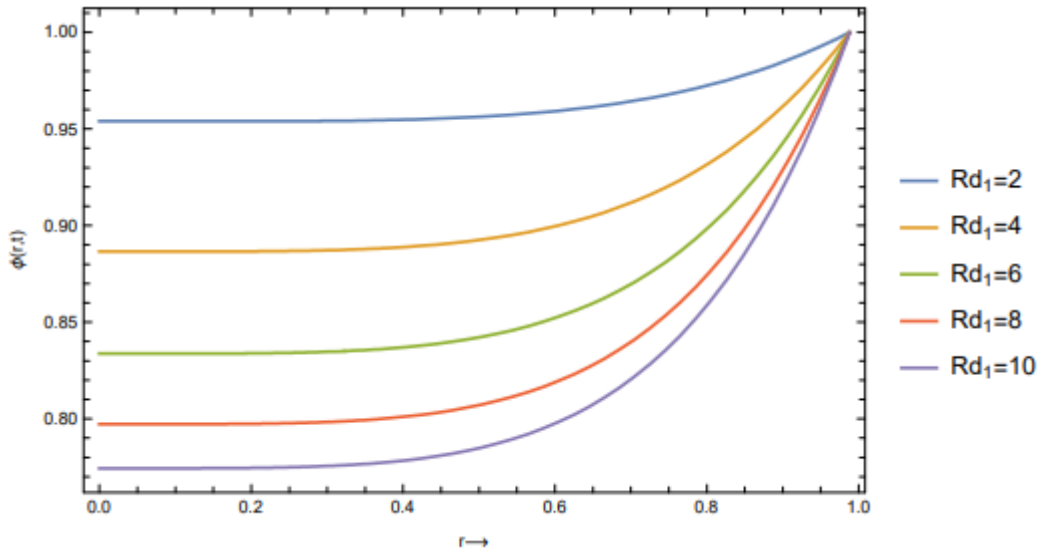

Fig 11. Plot Showing Cholesterol Concentration for Different Radiation with values

$Pr = 2.1, Sc = 0.2, \omega = 0.3, Sr = 2, x = 0.3$

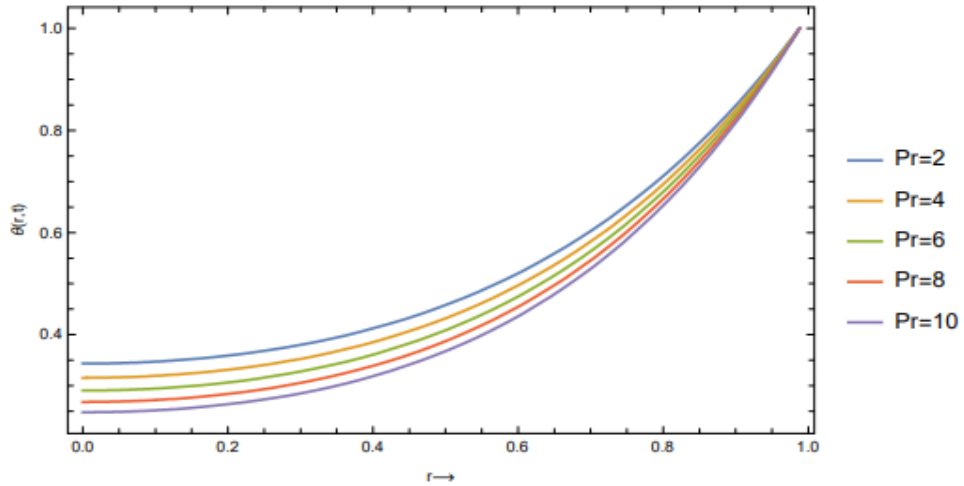

Fig 12. Plot Showing Blood Temperature for Different Prandtl Number with values

$Rd_1 = 2, \omega = 0.3, x = 0.3$

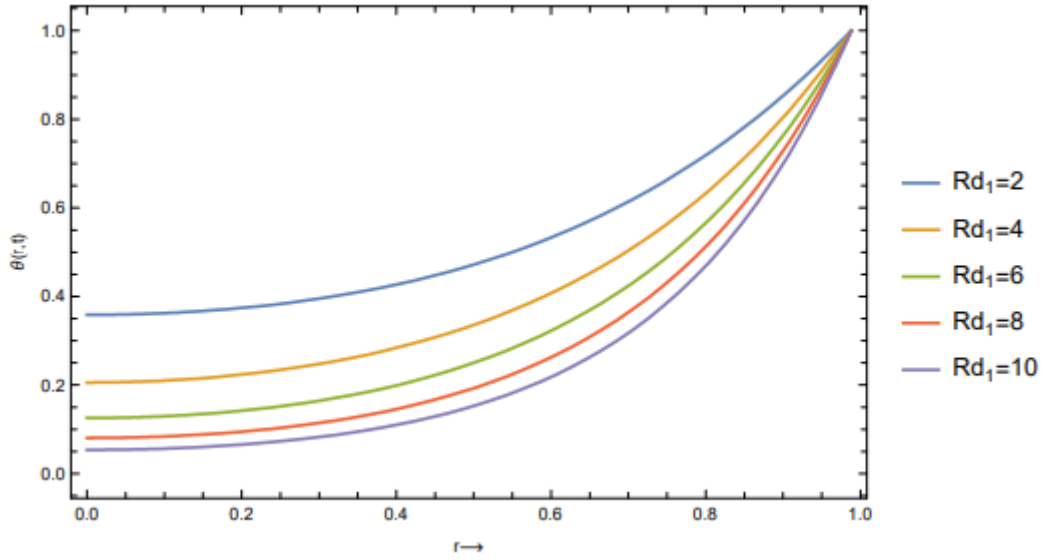

Fig 13. Plot Showing Blood Temperature for Different Radiation with values

$Pr = 2.1, \omega = 0.3, x = 0.3$

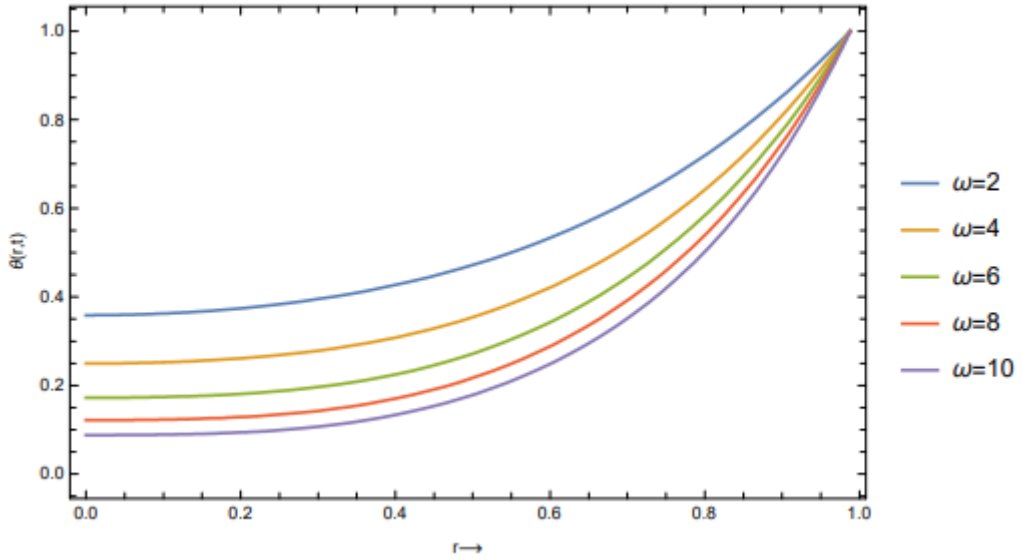

Fig 14. Plot Showing Blood Temperature for Different Oscillatory Frequency with values

$Pr = 2.1, Rd_1 = 2, x = 0.3$

DISCUSSION

Fig 1 illustrates the velocity of the blood flowing at a specific location in the stenotic region for several values of Soret number $Sr = 1, 2, 3, 4, 5$. In this result, the axial velocity increases with an increasing Soret number. Fig 2 elucidates the impact of solutal Grashof number on the blood flowing through a specific location $x = 0.3$ with other contribution parameters value $Sr = 2, Per = 2.1, Sc = 0.2, Rd_3 = 2, Rd_1 = 2, k = 0.05, M = 1.5$. In the figure, the velocity reduces with an increasing value of solutal Grashof number. The impact of Schmidt number on blood velocity at a specific location $x = 0.3$ was investigated and result shown in Fig 3. The result indicates a decrease in blood velocity for different values of Schmidt number, this result was supported with the introduction of the other pertinent parameter such as $Sr = 2, Gc = 15, Pr = 2.1, Rd_3 = 2, Rd_1 = 2, k = 0.05, M = 1.5$. Fig 4 depicts the impact of blood velocity for a change in Prandtl number. The figure shows that the blood velocity decreases for different unit increase of Prandtl number. However, Fig 5 illustrates an increase in blood velocity for different values of radiation. This is an indication that radiation increase is a good support in increasing blood velocity and it helps in blood thinning with the support of the other pertinent parameters $Sr = 2, Gc = 15, Pr = 2.1, Rd_3 = 2, k = 0.05, M = 1.5, \omega = 0.3$. Fig 6 illustrates blood velocity for different values of porosity at a specific location $x = 0.3$. The figure indicates that the velocity increases for an increase in units of porosity with other parameter values such as

$Sr = 2, Gc = 15, Pr = 2.1, \mathrm{Sc} = 0.2, Rd_3 = 2, Rd_1 = 2, k = 0.05, M = 1.5$

.

The study also investigated the impact of magnetic field on blood velocity, and it was found in Fig 7 that the velocity decreases for different units of magnetic field. The decrease in the velocity is caused by an increase in magnetic field and Lorentz force which inhibited the flow. This was also contributed by different units of the other pertinent parameters such as $Sr = 2, Gc = 15, Pr = 2.1, \mathrm{Sc} = 0.2, Rd_3 = 2, Rd_1 = 2, k = 0.05, M = 1.5$. Figs 8-11 indicate the impact of cholesterol concentration for different values of Soret number, Schmidt number, and Prandtl number and radiation parameter respectively. The figures indicate that the cholesterol concentration decreases for different units' increases in Soret number, Schmidt number, and Prandtl number and radiation parameter at a specific location $x = 0.3$. Finally, Figs 12-14 illustrate the importance of Prandtl number, radiation parameter and the oscillatory frequency on blood temperature. In the figures, it was found that the blood temperature decreases for different values of the aforementioned parameters.

CONCLUSION

The sclerotic effect on blood flow through an artery with heat on cholesterol concentration in the presence of a magnetic field was studied. Using the Laplace method, the governing nonlinear partial differential equations were solved and the influence of the effective parameters on the flow characteristics such as the velocity, cholesterol concentration, and temperature was examined. The results demonstrate that the axial velocity decreases with the increase in solutal Grashof number, Schmidt number, Prandtl number, and magnetic field on the blood velocity. However, the blood velocity increases with the increase in Soret number, radiation parameter, and porosity parameter. The Soret number, Schmidt number, Prandtl number, Oscillatory frequency, and radiation parameter increase caused the cholesterol concentration and blood temperature profile to decrease at a specific location at $x = 0.3$.

REFERENCES

1. Sharma, M., Sharma, B. K., Gaur, R. K., & Tripathi, B. (2019). Soret and Dufour effects in biomagnetic fluid of blood flow through a tapered porous stenosed artery. *Journal of Nanofluids*, *8*(2), 327-336.
2. Bunonyo, K. W., & Amos, E. (2020). Lipid concentration effect on blood flow through an inclined arterial channel with magnetic field. *Mathematical modelling and Applications*, *5*(3), 129.
3. Chakravarty, S., & Sannigrahi, A. K. (1999). A nonlinear mathematical model of blood flow in a constricted artery experiencing body acceleration. *Mathematical and computer modelling*, *29*(8), 9-25.
4. Abdollahzadeh Jamalabadi, M. Y., Daqiqshirazi, M., Nasiri, H., Safaei, M. R., & Nguyen, T. K. (2018). Modeling and analysis of biomagnetic blood Carreau fluid flow through a stenosis artery with magnetic heat transfer: A transient study. *PLoS One*, *13*(2), e0192138.
5. Haik, Y., Pai, V., & Chen, C. J. (2001). Apparent viscosity of human blood in a high static magnetic field. *Journal of Magnetism and Magnetic Materials*, *225*(1-2), 180-186.
6. Yadav, R. P., Harminder, S., & Bhoopal, S. (2008). Experimental studies on blood flow in stenosis arteries in presence of magnetic field. *Ultra Sci*, *20*(3), 499-504.
7. Sinha, A., Misra, J. C., & Shit, G. C. (2016). Effect of heat transfer on unsteady MHD flow of blood in a permeable vessel in the presence of non-uniform heat source. *Alexandria Engineering Journal*, *55*(3), 2023-2033.
8. Shit, G. C., & Roy, M. (2016). Effect of induced magnetic field on blood flow through a constricted channel: An analytical approach. *Journal of Mechanics in Medicine and Biology*, *16*(03), 1650030.
9. Barcroft, H., & Edholm, O. G. (1943). The effect of temperature on blood flow and deep temperature in the human forearm. *The Journal of physiology*, *102*(1), 5.
10. Sharma, B. K., Sharma, M., Gaur, R. K., & Mishra, A. (2015). Mathematical modeling of magneto pulsatile blood flow through a porous medium with a heat source. *International Journal of Applied Mechanics and Engineering*, *20*(2).
11. Faheti, D., Van der Zee, J., & Van Rhoon, G. C. (2009). Thermoradiotheraphy of cancer: an effective approach. *Australasian Medical Journal*, *2*(14).
12. Ma, P., Li, X., & Ku, D. N. (1994). Heat and mass transfer in a separated flow region for high Prandtl and Schmidt numbers under pulsatile conditions. *International journal of heat and mass transfer*, *37*(17), 2723-2736.
13. Sinha, A., & Shit, G. C. (2015). Electromagnetohydrodynamic flow of blood and heat transfer in a capillary with thermal radiation. *Journal of Magnetism and magnetic materials*, *378*, 143-151.
14. Sharma, M., & Gaur, R. K. (2017). Effect of variable viscosity on chemically reacting magneto-blood flow with heat and mass transfer. *Global Journal of Pure and Applied Mathematics*, *13*(3), 26-35.

15. Sharma, M., & Gaur, R. K. (2017). INTERNATIONAL JOURNAL OF ENGINEERING SCIENCES & RESEARCH TECHNOLOGY MODELING OF MHD BLOOD FLOW IN A BALLOON CATHETERIZED ARTERIAL STENOSIS WITH THERMAL RADIATION. 6(237).
16. Levin, W., Sherar, M. D., Cooper, B., Hill, R. P., Hunt, J. W., & Liu, F. F. (1994). Effect of vascular occlusion on tumour temperatures during superficial hyperthermia. *International journal of Hyperthermia*, *10*(4), 495-505.
17. Ponalagusamy, R., & Selvi, R. T. (2011). A study on two-layered model (Casson–Newtonian) for blood flow through an arterial stenosis: axially variable slip velocity at the wall. *Journal of the Franklin Institute*, *348*(9), 2308-2321.
18. Hanvey, R. R. ., & Bunonyo, K. W. (2022). Effect of Treatment Parameter on Oscillatory Flow of Blood through an Atherosclerotic Artery with Heat Transfer. *Journal of the Nigerian Society of Physical Sciences*, *4*(3),682. https://doi.org/10.46481/jnsps.2022.682
19. Hanvey, R. R. (2022). an Investigation of Blood Flow through Parallel Plate Channel in the Presence of Inclined Magnetic Field with Heat and Mass Transfer. *Trends in Sciences*, *19*(16), 5697. https://doi.org/10.48048/tis.2022.5697
20. Kubugha, B. W. ., & Amos, E(2022). Mathematical Modeling of LDL-C and Blood Flow through an Inclined Channel with Heat in the Presence of Magnetic Field. *Trends in Sciences*, *19*(16), 5693. https://doi.org/10.48048/tis.2022.5693
21. Bunonyo, K. W., & Ebiwareme, L. (2022). A Low Prandtl Number Haemodynamic Oscillatory Flow through a Cylindrical Channel using the Power Series Method. *European Journal of Applied Physics*, *4*(3), 56-65.
22. Nessa, A., Nooshin, R., Saman Ahmad, N., Ali, K., Alireza, F., & Yahya, D. (2017). Dermatology publications from Iran in MEDLINE: A comparison between 2004 and 2014. *Iranian Journal of Dermatology*, *20*(1), 15-20.

Nomenclature

x^*	Dimensional coordinate along the channel
r^*	Dimensional coordinate perpendicular to the channel
R	Radius of an abnormal channel
R_0	Radius of normal channel
P_0	Systolic pressure
Rd_1	Radiation parameter
Rd_3	Chemical reaction parameter
k_{Tb}	Blood thermal conductivity
w^*	Dimensional velocity profile
w	Dimensionless velocity profile
w_0	Perturbed velocity profile
C^*	Dimensional lipid particle concentration
C_∞	Far field cholesterol particle concentration
c_{bp}	The specific heat capacity of blood
t^*	Dimensionless time
T	Temperature of the fluid
T_∞^*	Far field temperature
T_w^*	Temperature at the wall
B_0	Magnetic field
M	Magnetic field parameter
a	Growth rate of LDL-cholesterol

Greek Symbols

υ_b	Kinematic viscosity of blood
μ_b	Dynamic viscosity of blood
Pr	Prandtl number for blood
g	Acceleration due to gravity
δ^*	Dimensional height of stenosis
σ_e	Electrical conductivity
λ^*	Length of stenosis
ω	Oscillatory frequency
θ	Dimensionless blood temperature
ϕ	Dimensionless cholesterol particle concentration
θ_a	Dimensionless wall temperature
θ_0	Perturbed blood temperature profile
ϕ_a	Dimensionless wall lipid concentration
ϕ_0	Perturbed lipid concentration
ρ_b	Blood density

Subscripts

w	Wall
b	Blood
e	Electrical
T	Thermal
∞	Far field

MMDARG Mathematical Modeling and Data Analytic Research Group

Appendix

$$J_0\left(i\beta_1 r\right)=I_0\left(\beta_1 r\right)$$

$$\beta_1^2=\left(\frac{1}{k}+M^2+i\omega\right),\beta_2^2=\left(Rd_1+i\omega\right)Pr,\beta_4^2=Sci\omega$$

$$A_0=\left(\frac{e^{i\omega t}}{I_0\left(\beta_4 h\right)}-\frac{A_1}{I_0\left(\beta_4 h\right)}-\frac{A_2h^2}{I_0\left(\beta_4 h\right)}-\frac{A_3h^4}{I_0\left(\beta_4 h\right)}\right),P_1=P_0-A_1Gc$$

$$A_1=\frac{\beta_2^2S_rSce^{-i\omega t}}{I_0\left(\beta_2 h\right)}+\left(\frac{\beta_2^4S_rSce^{-i\omega t}}{\beta_4^4I_0\left(\beta_2 h\right)}+\frac{\beta_2^6S_rSce^{-i\omega t}}{\beta_4^6I_0\left(\beta_2 h\right)}\right),A_2=\frac{\beta_2^4S_rSce^{-i\omega t}}{4\beta_4^2I_0\left(\beta_2 h\right)}+\frac{\beta_2^6S_rSce^{-i\omega t}}{4\beta_4^4I_0\left(\beta_2 h\right)},$$

$$A_3=\frac{\beta_2^6S_rSce^{-i\omega t}}{64\beta_4^2I_0\left(\beta_2 h\right)},B_3=-\frac{A_4}{I_0\left(\beta_1 h\right)}-A_5\frac{I_0\left(\beta_2 h\right)}{I_0\left(\beta_1 h\right)}-A_6\frac{I_0\left(\beta_4 h\right)}{I_0\left(\beta_1 h\right)}-\frac{A_7h^2}{I_0\left(\beta_1 h\right)}-\frac{A_8h^4}{I_0\left(\beta_1 h\right)}$$

$$A_4=4\left(\frac{A_2Gc}{\beta_1^4}+\frac{16A_3Gc}{\beta_1^6}\right)-\frac{P_1}{\beta_1^2},A_5=\left(\frac{Gre^{-i\omega t}}{\beta_1^2I_0\left(\beta_2 h\right)}\right),A_6=\frac{GcA_0}{\beta_1^2},A_7=\left(\frac{A_2Gc}{\beta_1^2}+\frac{16A_3Gc}{\beta_1^4}\right)$$

$$I_0\left(\beta_4 r\right)=\left(1+\frac{\beta_4^2r^2}{4}+\frac{\beta_4^4r^4}{64}+\frac{\beta_4^6r^6}{2304}+\ldots\right),A_3=\frac{\beta_2^6S_rSce^{-i\omega t}}{64\beta_4^2I_0\left(\beta_2 h\right)},A_8=\frac{A_3Gc}{\beta_1^2}$$

$$A_1=\frac{\beta_2^2S_rSce^{-i\omega t}}{I_0\left(\beta_2 h\right)}+\left(\frac{\beta_2^4S_rSce^{-i\omega t}}{\beta_4^4I_0\left(\beta_2 h\right)}+\frac{\beta_2^6S_rSce^{-i\omega t}}{\beta_4^6I_0\left(\beta_2 h\right)}\right),A_2=\frac{\beta_2^4S_rSce^{-i\omega t}}{4\beta_4^2I_0\left(\beta_2 h\right)}+\frac{\beta_2^6S_rSce^{-i\omega t}}{4\beta_4^4I_0\left(\beta_2 h\right)}$$

$$I_0\left(\beta_2 r\right)=\left(1+\frac{\beta_2^2r^2}{4}+\frac{\beta_2^4r^4}{64}+\frac{\beta_2^6r^6}{2304}+\ldots\right),\text{ and }I_1\left(\beta_2 r\right)=\left(\frac{2\beta_2^2r}{4}+\frac{4\beta_2^4r^3}{64}+\frac{6\beta_2^6r^5}{2304}+\ldots\right)$$

$$I_1'\left(\beta_2 r\right)=\left(\frac{2\beta_2^2}{4}+\frac{12\beta_2^4r^2}{64}+\frac{30\beta_2^6r^4}{2304}+\ldots\right)\text{ and }I_0\left(\beta_2 h\right)=\left(1+\frac{\beta_2^2h^2}{4}+\frac{\beta_2^4h^4}{64}+\frac{\beta_2^6h^6}{2304}+\ldots\right)$$